

Chapter 6

Fluorinated Polyhedral Oligosilsesquioxane Surfaces and Superhydrophobicity

Scott T. Iacono, Andrew J. Peloquin, Dennis W. Smith, Jr. and Joseph M. Mabry

6.1 Introduction

Fluorinated compounds are a logical choice for hydrophobic applications owing to their generally low surface energy. Polyhedral molecules may also improve hydrophobicity by increasing material surface roughness. There have been many recent attempts to synthesize and characterize various types of fluorinated polyhedra. These reports include the fluorination or fluoroalkylation of C_{60} [1,2]. Unfortunately, $C_{60}F_{48}$ (fluorinated buckminsterfullerene) cannot be used as a hydrophobic material, since it is metastable and is hydrolyzed by water [3]. However, the perfluorocarborane species, perfluoro-deca- β -methyl-*para*-carborane, shows remarkable hydrolytic and oxidative stability [4]. Fluorinated carbon nanotubes and nanofibers have also been produced [5]. Many of these fluorinated polyhedral compounds may be useful in hydrophobic applications, but they are generally hazardous to prepare, require air and moisture sensitive manipulations, and have limited economies of scale. For these reasons, alternative fluorinated polyhedra, such as Polyhedral Oligomeric Silsesquioxanes (POS) are highly desired (Figure 6.1).

Scott T. Iacono
U.S. Air Force Academy, Department of Chemistry, USAF Academy, Colorado Springs, CO 80840,
USA

Andrew J. Peloquin
U.S. Air Force, Patrick AFB, FL 32925, USA

Dennis W. Smith, Jr.
Department of Chemistry & Center for Optical Materials Science & Engineering Technologies,
Clemson University, Clemson, SC 29634, USA

Joseph M. Mabry
Air Force Research Laboratory, Space & Missile Propulsion Division, Edwards AFB, CA 93524, USA
E-Mail: joseph.mabry@edwards.af.mil

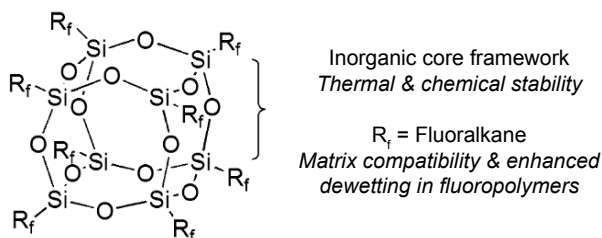


Fig. 6.1 General structure of fluorinated polyhedral oligomeric silsesquioxanes

The addition of fillers to polymeric matrices is of extreme technological importance (see also Chapter 5). Filler addition can impart enhanced scratch resistance, increase thermal or mechanical properties, and improve processing parameters. Silicate and carbon black based fillers are quite common. They are often inexpensive and their incorporation into many polymer systems is fairly straightforward. When miscibility is a problem, surface modification of the fillers to further enhance their compatibility is widespread. The silylation of surface silanol groups on silica fillers is a good example. Processing is another factor that has been optimized. The use of high shear to break up large agglomerates or aggregates of nanoscopic particles is common. These approaches yield nanoscopic species with large surface areas, which should favor physisorption and/or chemisorption between the polymer chain and the filler.

Polyhedral Oligomeric Silsesquioxanes (POS) are thermally robust cages consisting of a silicon-oxygen framework, most commonly possessing alkyl functionality on the periphery. POS have been used in the development of high performance materials for commercial aerospace and medical applications [6,7] (see also Chapters 8 and 9 respectively). POS molecules can be functionally tuned, are easily synthesized with inherent functionality, and are often commercially available [8]. POS compounds may possess a high degree of compatibility in blended polymers and can easily be covalently linked into a polymer backbone [9]. The incorporation of POS into polymers often produces nanocomposites with more desirable properties, such as higher glass transition temperature, mechanical strength, thermal and chemical resistance, and ease of processing. Applications include space-survivable coatings [10,11] and ablative and fire-resistant materials [12–14]. POS can be produced as either completely condensed cages or incompletely condensed cages with silanol groups that allow further modification. Owing to its physical size, the incorporation of POS into polymers generally serves to reduce polymer chain mobility, often improving both thermal and mechanical properties.

A number of recent reports have detailed POS materials as reinforcing fillers (or reinforcing co-monomers) in a number of composite systems with nanometer-sized domains [15–17]. The results reported herein are somewhat different, in that the monodisperse POS building blocks seem to be rather non-interacting. Specifically, the organic functionality surrounding the silsesquioxane core is composed of fluorinated alkyl groups. Fluoroalkyl compounds are known to be basically inert. This is largely because they are non-polarizable and have low surface free energies.

Fluoroalkyl chains are often rigid, due to steric and electronic repulsion. This large corona of the fluorinated POS compounds should help retard the van der Waals attraction between POS cores. These POS materials are monodisperse and crystalline. The melting point of the POS is lower than the processing conditions of various fluoropolymers, so one can safely assume that hard filler effects should not be an issue during melt blending. In this regard, one may expect that these materials could exhibit small molecule, solvent like, characteristics. This paper discusses many of the parameters and physical properties of simple blends of fluorinated POS materials in fluoropolymer matrices. It is demonstrated that these simple blends do not rigorously correspond to idealized filled polymer models, or to solvent swollen systems. Herein, we describe the properties resulting from the blending of these fluorinated POS compounds into various fluoropolymers.

6.2 Experimental

6.2.1 *Materials*

Fluorinated POS compounds **FH**, **FO**, **FD** (Fig. 6.2) and the corner-capped series **2–9** (Fig. 6.3) were prepared and fully characterized from previously published procedures [18,19]. **6F-BP** PFCB aryl ether polymer (Fig. 6.7, $M_n = 22,000–25,000$) was donated and is also commercially available from Tetramer Technologies, L.L.C. and distributed through Oakwood Chemicals, Inc. Polychlorotrifluoroethylene (PCTFE or Neoflon M 400-H) was obtained from Dai-kin. Hexadecane, and hexafluorobenzene were purchased through Aldrich and used without further purification.

6.2.2 *Single Crystal X-Ray Structural Characterization*

Crystal data for **FH** and **FD** POS were collected at $T = 103.0(2)$ K using Bruker 3-circle, SMART APEX CCD with χ -axis fixed at 54.74° , running on SMART V 5.625 program (Bruker AXS: Madison, WI, 2001). Crystallographic data for all structures have been deposited in the Cambridge Crystallographic Data Center (CCDC). Assigned CCDC numbers for **FH** and **FD** are 608207 and 608209, respectively. Copies of the crystallography data can be obtained, free of charge, from CCDC, 12 Union Road, Cambridge CB2 1EZ, UK (e-mail: deposit@ccdc.cam.ac.uk).

6.2.3 *Fluorinated POS Coating and Composite Preparation*

6.2.3.1 Spin Cast Fluorinated POS Coating

POS powder surfaces were prepared by dissolving the fluoroalkyl POS in a minimal amount of hexafluorobenzene followed by mechanical agitation. The surfaces were spin cast at 2500 RPM onto borosilicate glass plates producing a well-adhered coating.

6.2.3.2 Fluorinated POS Solvent Blended Composites with 6F-BP PFCB Aryl Ether Polymer

Two methods were used to prepare polymer (or blend) films. For spin cast films, the dried polymer is initially applied in a minimal amount of THF onto a glass substrate, and then spin coated at 2500–3000 RPM using a Chemat KW-4A spin coater. The polymer-coated substrate is dried in a vacuum oven at 60 °C for 24 h. For drop-cast films, the polymer dissolved in a minimal amount of THF was dispensed onto a glass plate to uniformly coat the surface. The polymer solution was allowed to evaporate in a glass enclosure for 48 h and then finally dried in an oven at 60 °C for an additional 24 h. Spin and drop-cast films were approximately 1–2 μm thick and were measured by the Zygo NewView 6300 3D white light optical profiling system.

6.2.3.3 Fluorinated POS Melt Blended PCTFE

Fluoropolymer composites are prepared by adding the designated wt % of **FD** and **FO** POS melt blended into PCTFE. Melt processing and blending of POS/fluoropolymers was conducted on a DSM Micro 5 Compounder having a chamber free volume of 5 cm³. Powders were pre-mixed in their appropriate ratios and charged to the mixer, imposing a residence time of 5 min under an inert nitrogen atmosphere with the modular heating profile set at a flat 280 °C. Blend extrudates were transferred to a DSM micro-injection molding machine for the fabrication of disks. Samples for dynamic mechanical thermal analysis (DMTA), contact angle measurements, and atomic force microscopy (AFM) were thin films. The films were made by compression molding two grams of the polymer-blend extrudate utilizing a Tetrahedron compression molder. The bars for SEM were also compression molded with the same molding times and temperatures, but utilizing only ½ ton of force.

6.2.4 *Thermo-Mechanical Analysis*

The compression molded films were cut into 3×20 mm rectangular samples for dynamic mechanical thermal analysis utilizing a DMTA V from TA Instruments. All fluoropolymer samples were analyzed using a 5 °C temperature ramp and a tensile geometry. The PCTFE samples were each tested from 30 °C to 150 °C. Stress/strain tests were performed on all samples to identify the largest force at which the material exhibited an elastic deformation, thus limiting the pre-tension force used to test the samples. Strain sweeps were also performed to ensure that the testing strain was within the linear viscoelastic region. The Fluorinated POS effect on the thermal stability of the fluoropolymers was examined using a 2050 TGA from Rheometric Scientific in the presence of nitrogen.

6.2.5 *Microscopy*

The dispersion of the fluorinated POS was investigated using atomic force microscopy (AFM) and scanning electron microscopy (SEM).

6.2.5.1 **Atomic Force Microscopy (AFM)**

The AFM measurements were performed in tapping mode using a Digital Instruments Dimension 3100 Scanning Probe Microscope (SPM), which utilizes automated atomic force microscopy (AFM) and scanning tunneling microscopy (STM) techniques. Atomic Force Microscopy was conducted on a Nanoscope IV controller (3100 SPM Head) in tapping mode. Etched Silicon probes of nominal spring resonance 300 kHz (spring constant approx. 0.3 mN m^{-1}) were used for light tapping (driving amplitude ca 1.1 V) of varying section size at 1-2 Hz collection times (512 points/line). For melt-processed samples, the AFM samples were cut from the compression molded films discussed in the results and discussion section. It was noted that most of the surfaces did not have a significant phase image, which was interpreted as being indicative of relatively uniform surfaces that differed only in surface topography. The surface roughness was dominated by the processing effects, e.g., gross striations indicative of film buckling upon removal. However, fine scale features were resolvable and will be discussed. In the AFM micrograph images, height is shown on the left side of the figure and a simultaneously collected phase image is shown on the right.

6.2.5.2 **Scanning Electron Microscopy (SEM)**

Scanning electron microscopy was performed using an ISI CL6 operating at 15

keV equipped with a Kevex X-ray detector. Elemental mapping was performed using energy dissipation X-ray analysis with IXRF Systems analysis software. Samples were cut from compression molded bars and the cross-section was imaged. Furthermore, an elemental mapping of the surface is discussed.

6.2.6 *Static and Dynamic Contact Angle*

Contact angle analyses were performed on a FDS Dataphysics Contact Analyzer System using a syringe metering pump. Deionized water (18 M Ω ·cm, Barnstead) was used as the interrogating liquid. Small drops of water (approximately 2-5 μ l) were accurately metered onto a flat surface, and the full screen image of the drop was captured with the frame grabbing software coupled to a CCD camera operating at the optimized zoom and contrast. The contact angles were determined via the software suite or via graphical fitting of the contact tangents in the captured image. Both approaches gave the same nominal value within ± 2 degrees. Static water contact angle values reported were an average of three values measured on various areas of the surface.

6.3 Results and Discussion

6.3.1 *Fluorinated POS Synthesis*

Fluorinated POS compounds fluorodecyl (**FD**), fluorooctyl (**FO**), and fluoroheptyl (**FH**) were produced by the base-catalyzed hydrolysis of trialkoxy silanes (Figure 6.2). These compounds tend to condense into T₈ cages, rather than cage mixtures, as has been previously observed in the base-catalyzed synthesis. The yields for these reactions are often nearly quantitative. This is significant because the usual method to produce T₈ cages is the acid-catalyzed hydrolysis of trichlorosilanes, which produces an undesirable acidic by-product.

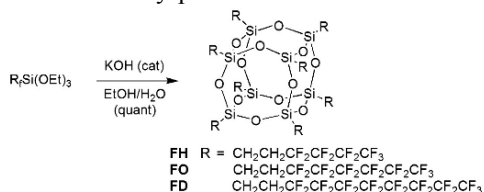


Fig. 6.2 Direct synthesis of octahedral fluorinated POS compounds

Hepta(3,3,3-trifluoropropyl)tricycloheptasiloxane trisodium silanolate **1** was used as an intermediate for the preparation of fluorinated POS compounds **2–7**

by “corner-capping” with fluoroalkyltrichlorosilanes (Figure 6.3). The intermediate salt (**1**) is stable in air, but decomposes to silsesquioxane resin upon exposure to moisture. The intermediate adduct is the result of a pathway to fully

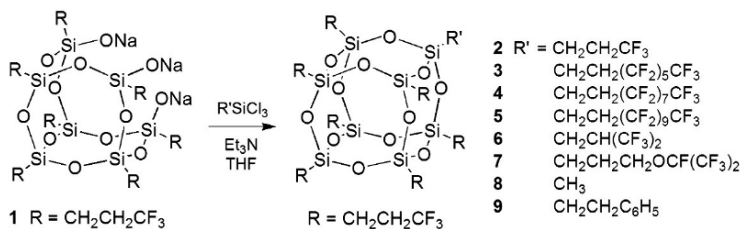


Fig. 6.3 Synthesis of corner-capped fluorinated POS compounds

condensed cage structures by simply controlling feedstock stoichiometry.

Corner-capping with commercially available functionalized fluoroalkyltrichlorosilanes afforded diverse structures with linear fluoroalkyl chains (**2–5**), a branched hexafluoroisopropyl (**6**), and a heptafluoroisopropoxypropyl ether (**7**). Fluorinated POS **2** (synonymously denoted **FP** for fluoropropyl) possesses octahedral symmetry like those fluorinated POS series **FH**, **FO**, and **FD**. This corner-capping methodology was employed in the incorporation of methyl (**8**) and phenylethyl (**9**) hydrocarbon groups in the predominantly fluorinated environment.

6.3.2 Fluorinated POS Properties

Selected properties of fluorinated POS compounds are illustrated in Table 6.1. These Fluorinated POS compounds are only soluble in fluorinated solvents such as AK-225G (Asahi Glass) and hexafluorobenzene. Unlike most non-fluorinated POS compounds, thermogravimetric analysis (TGA) indicates fluorinated POS volatilize rather than decompose. No residue remains after heating under either nitrogen or dry air. **FD** POS is the most stable compound, subliming at over 300 °C. Fluorinated POS are also very dense, high molecular weight materials. For example, **FD** POS has a molecular weight of 3993.54 g mol⁻¹ and a density of 2.067 g cm⁻³.

The structure–property relationships for fluorinated POS compounds were studied from experimental melting points (T_m) obtained from the amorphous powders precipitated from methanol. As a general trend, melting points become depressed as fluoroalkyl chain lengths increase due to weaker intermolecular van der Waals attractions. All fluorinated POS compounds were observed to possess narrow melting points as high molecular weight compounds, indicative of high purity (Table 6.1). In all cases, no decomposition was observed for these compounds at the melting point. It is clear from the data in Table 6.1 that melting point properties are primarily influenced by substrate structure and not solely by

wt % F content. In this case, the low melting points of extended fluorinated POS compounds **3–5** would be valuable in the low temperature melt processing of polymers, affording blended composites.

The fluorinated POS compounds were spin-cast from hexafluorobenzene onto a glass substrate. The spin-casting produced well-adhered, white powder-like films, and did not visually expose any of the glass substrate. Their static (or advancing) contact angles were measured using deionized water and hexadecane as test fluids. Hexadecane is a standard test fluid for determining the oil repellency (or oleophobicity) of a material. The fluorinated POS series measured water contact angles are on average 50° higher than for hexadecane contact angles. As a consequence of the highest wt % F content, **FD** produced the highest water and hexadecane static contact angles, of 154° and 87° respectively. Since its water contact angle was greater than 150°, the surface of **FD** as a spin cast powder was formally classified as being ultrahydrophobic.

For the fluorinated POS octamer series of **FP**, **FH**, **FO** and **FD**, there is a near linear progression of water and hexadecane contact angle in relation to the increasing fluorine content of the fluorinated POS compounds. This is clearly shown by a 13% increase in water contact angle from **FP** (38.2% fluorine content) to the **FH** (57.2% fluorine content) compound. A leveling-off effect is anticipated for the series for fluoroalkyl substitution beyond the **FO**, since a negligible increase of 5% was observed from **FH** (57.2% fluorine content) to **FO** (61.9% fluorine content). However, the **FD** (64.7% fluorine content) showed an abrupt increase of 12% relative to **FO** POS. A similar trend was observed for hexadecane contact angles, but the standard deviation would indicate that the oleophobicities of **FH**, **FO**, and **FD** are the same.

Table 6.1 Selected properties of fluorinated POS compounds

| Compound | Fluoroalkyl group | $\theta_{\text{water}}/^\circ$ | $\theta_{\text{hex}}/^\circ$ | $T_m/^\circ\text{C}^a$ | wt % F ^b |
|----------|---|--------------------------------|------------------------------|------------------------|---------------------|
| FP (2) | R = R' = CH ₂ CH ₂ CF ₃ | 116 | 69 | 234-237 | 38.5 |
| FH | R = CH ₂ CH ₂ (CF ₂) ₃ CF ₃ | 131 | 80 | 121-123 | 57.2 |
| FO | R = CH ₂ CH ₂ (CF ₂) ₅ CF ₃ | 138 | 82 | 120° | 61.9 |
| FD | R = CH ₂ CH ₂ (CF ₂) ₇ CF ₃ | 154 | 87 | 150° | 64.7 |
| 3 | R = CH ₂ CH ₂ CF ₃ R' = CH ₂ CH ₂ (CF ₂) ₅ CF ₃ | 109 | 77 | 104-106 | 45.0 |
| 4 | R = CH ₂ CH ₂ CF ₃ R' = CH ₂ CH ₂ (CF ₂) ₇ CF ₃ | 112 | 76 | 88-90 | 50.5 |
| 5 | R = CH ₂ CH ₂ CF ₃ R' = CH ₂ CH ₂ (CF ₂) ₉ CF ₃ | 112 | 80 | 105-107 | 51.8 |
| 6 | R = CH ₂ CH ₂ CF ₃ R' = CHCH(CF ₃) ₂ | 122 | 74 | 234-236 | 40.9 |

| Compound | Fluoroalkyl group | $\theta_{\text{water}}/^\circ$ | $\theta_{\text{hex}}/^\circ$ | $T_m/^\circ\text{C}^a$ | wt % F ^b |
|----------|--|--------------------------------|------------------------------|------------------------|---------------------|
| 7 | R = CH ₂ CH ₂ CF ₃ R' = CH ₂ CH ₂ CH ₂ OCF(CF ₃) ₂ | 108 | 73 | 70-71 | 40.4 |
| 8 | R = CH ₂ CH ₂ CF ₃ R' = CH ₃ | 102 | 51 | 168-170 | 35.9 |
| 9 | R = CH ₂ CH ₂ CF ₃ R' = CH ₂ CH ₂ C ₆ H ₅ | 106 | 45 | 109-111 | 33.0 |

^aMelting point capillary. ^bCalculated from molecular formula. ^cDSC analysis at midpoint.

Generation of potential energy surfaces for a packed lattice of **FH** (Figure 6.4) and **FD** (Figure 6.5) provided a better understanding of the increase in water contact angle observed for **FD** POS. **FD** POS appears to exhibit a molecular roughening arranged in a corrugated fashion. **FP** and **FO** POS appear similar to the flatter **FH** POS. This increased molecular-scale, surface roughness presumably contributes to the dramatic increase in the water contact angle of **FD** to 154°, which is approximately 23° higher than **FH**.

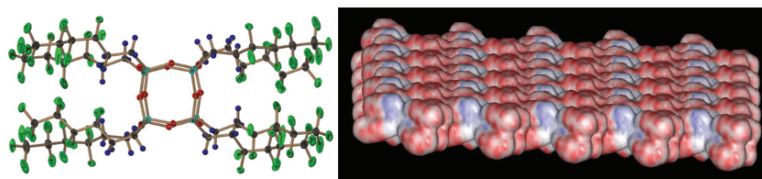


Fig. 6.4 X-ray crystal structure (left) and electrostatic potential diagram of FH POS (right) exhibiting a relatively flat surface

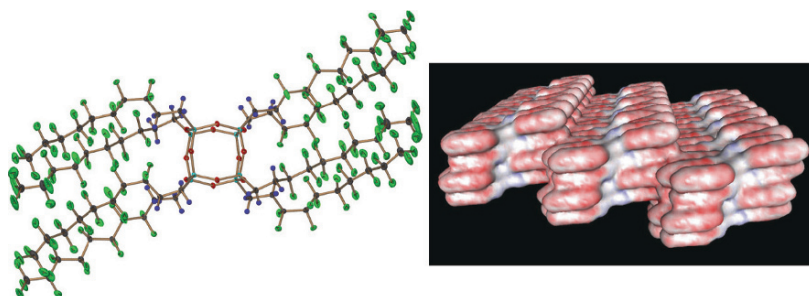


Fig. 6.5 X-ray crystal structure (left) and electrostatic potential diagram of FD POS (right) exhibiting a corrugated type surface

The potential energy surfaces shown in Figure 6.4 and Figure 6.5 represent crystalline surfaces obtained by single crystal X-ray analysis. It should be noted that the water contact angles for the observed trend were analyzed from spin cast, semicrystalline powder films. AFM analysis revealed the spin cast **FD** POS surface produced a root mean square (rms) roughness of approximately 4 μm (Figure 6.6).

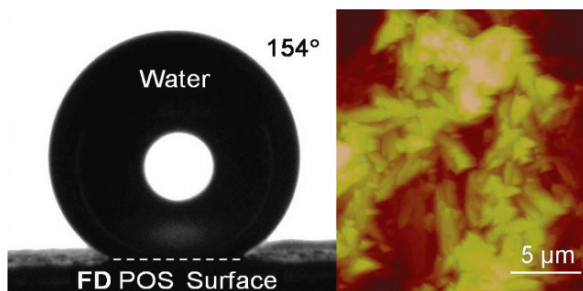


Fig. 6.6 Goniometer image of water drop on spin cast film (SCF) of FD POS with a measured contact angle of 154° (left) and AFM height image (right) of SCF of FD POS showing micrometer-size crystalline aggregates

6.3.3 POS Fluoropolymers

Selected fluorinated POS compounds possessing the highest hydrophobicity and oleophobicity were blended into several fluoropolymers in a preliminary study of fluorinated POS compatibility in polymer matrices. For the purposes of this study, **FD POS 6F-BP** perfluorocyclobutyl (PFCB) aryl ether (Figure 6.7) polymer blends are used to describe fluorinated POS dispersion and its effect on surface wettability (Section 6.3.3.1), and **FO** and **FD POS** blends in commercial PCTFE are used to describe melt processing (Section 6.3.3.2), thermo-mechanical (Section 6.3.3.3), and surface properties (Section 6.3.3.4).

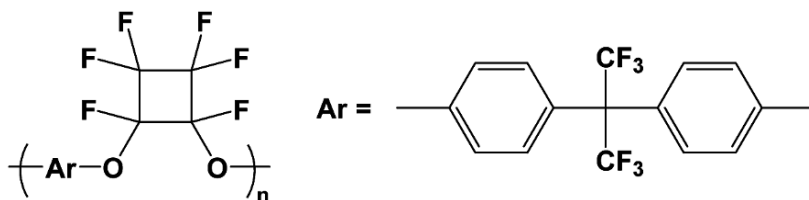


Fig. 6.7 6F-Biphenyl (6F-BP) perfluorocyclobutyl (PFCB) aryl ether polymer

6.3.3.1 Dispersion

The level of dispersion of fluorinated POS compounds into polymer systems is largely dependent on surface chemistry. PFCB aryl ether polymers are of interest in a multitude of materials applications, especially for their ability to produce optically transparent and processable films [20]. Increasing **FD POS** wt % loadings blended with **6F-BP** PFCB aryl ether polymer showed a gradual increase in water contact angle, but a significant increase in hexadecane contact angle (Figure 6.8). The **6F-BP** PFCB aryl ether polymer is intrinsically hydrophobic and produced water and

hexadecane contact angles of 95° and 27° , respectively. **FD POS** loadings up to 15 wt % developed a plateau from static water contact angle; the blend showed an overall 32% increase in water contact angle (124°) at this loading compared with unblended **6F-BP**. At optimized **FD POS** loadings of 10 wt %, a maximum hexadecane contact angle of 80° was observed, increasing hexadecane repellency by 158%. While films prepared with 15 wt % **FD POS** loading still appeared transparent and homogenous, 20 wt % **FD POS** produced slight phase separation. At 30 wt % **FD POS**, significant incompatibility was observed, producing brittle opaque films with crystalline aggregates on the film surface.

It was notable that when blended surfaces were tilted beyond 90° or even inverted (180°), water remained pinned to the film; this is not the case with powdered surfaces solely prepared from spin cast fluorinated POS. A surface with a contact angle of 90° or higher is considered a “non-wetting” surface, while a surface with a contact angle below 90° is considered “wetting.” Addition of fluorinated POS yielded “non-wetting” surfaces.

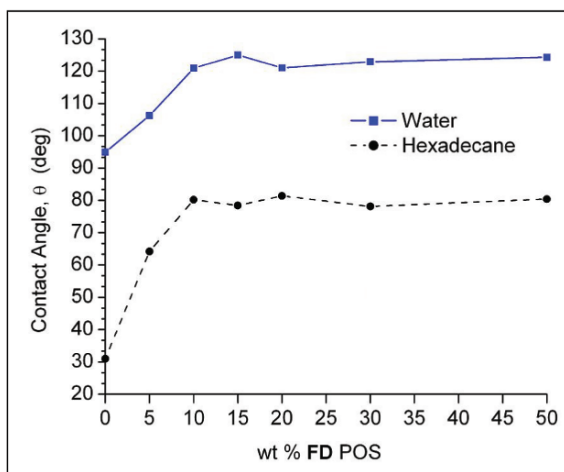


Fig. 6.8 Water and hexadecane contact angles of various wt % of **FD POS** blended into **6F-BP PFCB** aryl ether polymer

Dynamic water and hexadecane contact angles were evaluated to determine the degree of hysteresis of **FD POS** blended into **6F-BP PFCB** aryl ether polymer. The angles of advancing (θ_a) and receding (θ_r) of water and hexadecane were obtained by placing a liquid drop on the surface and tilting the stage of the goniometer. The results of the measurements for water and hexadecane are shown in Figure 6.9. At all wt % of **FD POS** blended into the polymer, the water and hexadecane drops remained pinned on the surface, even when the stage was tilted 90° . Initially, the advancing and receding angles were taken at the onset of liquid drop perturbation on the uphill and downhill side as the stage was tilted. However, these measurements were difficult to assess “by eye” and produced a high deviation in recorded values. Therefore, the dynamic angles were recorded at a 90° tilt in order

to ensure consistency. These results indicate a condition of high surface hysteresis where the surface energy (γ_{SV}) exceeds the surface tension (γ_{SL}) of the liquid drop.

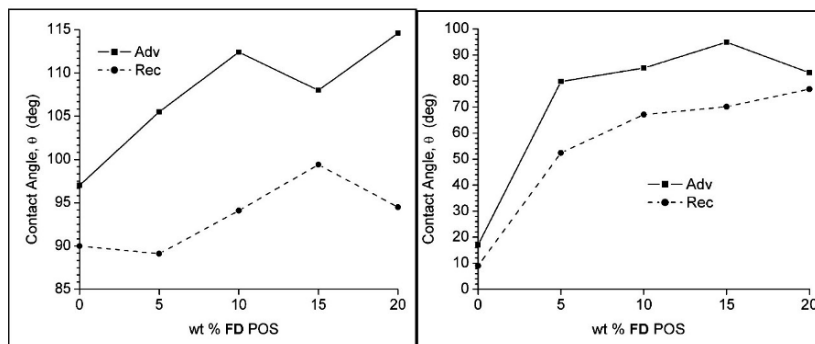


Fig. 6.9 Dynamic water (left) and hexadecane (right) contact angles of various wt % of FD POS blended into 6F-BP PFCB aryl ether polymer

Blending **FD POS** into the **BP-6F PFCB** aryl ether polymer introduced additional fluorine content and increased surface roughness. The relationship between contact angle and surface energy is governed by Young's equation, which relates surface interfacial tensions to the liquid and gas phases of water [21]. Furthermore, surface roughness imparts increased hydrophobicity to a material, as demonstrated by Cassie and Baxter, as well as Wenzel [22,23].

Atomic force microscopy (AFM) analysis of 15 wt % **FD** blend (Figure 6.10) compared with the virgin **6F-BP PFCB** aryl ether polymer (Figure 6.11) showed a marked increase in surface roughness. From AFM analysis, unblended **6F-BP** polymer and 15 wt % **FD POS** composite blend gave measured surface roughnesses of 0.527 nm and 1.478 nm, respectively. The incorporation of the fluorinated **FD POS** structures produced this threefold increase in surface roughness, possibly caused by blooming and aggregation of these structures on the surface during the spin-casting process. The increase in surface roughness was nearly 1 nm (the difference between 1.278 nm and 0.527) owing to the inclusion of **FD POS**. Such a slight increase in surface roughness is usually not enough to influence the overall macroscopic properties such as the contact angle. It is generally accepted that average surface roughness (R_a) < 100 nm has little effect on contact angles and hysteresis. Therefore, it is presumed that the low surface energy fluorine content contributed by fluorinated POS has the most influence on the surface contact angle, whereas the surface roughness is an important, but minor contributing parameter. On-going surface characterization is being investigated in order to determine the concentration gradient of the fluorinated POS structures on the surface compared to those entrained in the bulk material.

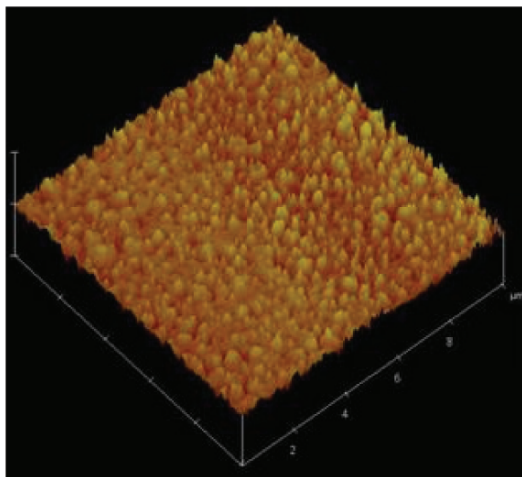


Fig. 6.10 AFM height image of **6F-BP** PFCB aryl ether polymer with 15 wt % **FD POS**

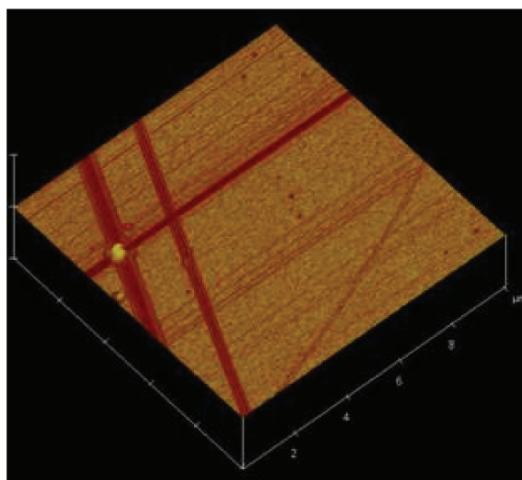


Fig. 6.11 AFM height image of **6F-BP** PFCB aryl ether polymer

6.3.3.2 Melt Processability

The processability of the samples was compared using torque and load of the compounder motor, a measure of the pressure generated in the mixer, where the pressure is generated as a result of the conical design of the mixer. For a constant volume of material compounded, and a fixed screw speed, the pressure generated is proportional to the viscosity of the material. The lower the pressure, the lower the viscosity, and the easier the material is to process. The second measure of

processability is the torque output by the motor. This gives an indication of the mechanical energy put into the system, and is proportional to the current used by the motor. Hong et al. utilized a similar measure to characterize the processability of polyethylene and hyperbranched polymer blends [24]. The lower the torque output the more processable the polymer (for a given screw speed).

These two measures of the processability of the polymer blends were recorded at 30 s intervals during processing. It was found that within a 95% confidence interval, the load and torque values were constant for the duration of processing, excluding the first 30 s. Therefore, an average value for both torque and load is assigned to each processing run. In order to investigate the effect of the addition of fluorinated POS, relative torque and relative load values were computed utilizing the average values in comparison to the average values found for the unfilled resins. Figure 6.12 shows the relative torque and load values with respect to the wt % of POS added for the PCTFE blends. The solid symbols represent the relative torque values, and the relative load results are illustrated by the open symbols. The square symbols denote the results of the **FD** POS blends, and the circular symbols denote the **FO** POS blend results. One will note that PCTFE processability is improved by more than 30%.

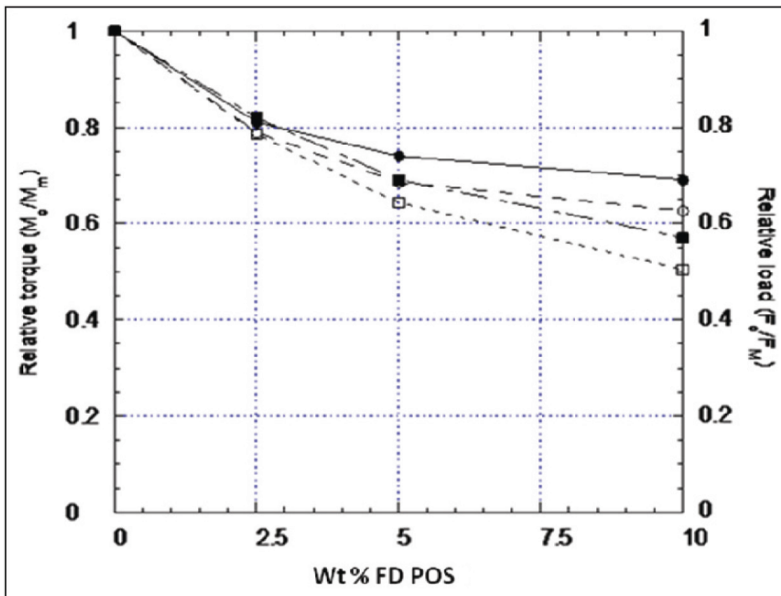


Fig. 6.12 Effect of FD POS on processing variables torque and load for PCTFE blends

6.3.3.3 Thermo-Mechanical Analysis

In order to determine the effect of the fluorinated POS on the mechanical properties

of PCTFE, dynamic mechanical analysis (DMA) was performed. Figure 6.13 illustrates the storage and loss moduli for the PCTFE blends. Notice only a small decrease in the modulus values between the filled and unfilled samples. The loss moduli of the PCTFE blends are very similar in value to the unfilled PCTFE, with only a slight decrease. The mechanical properties of the fluoropolymer are only slightly altered by the addition of fluorinated POS. The possible exception to this is the composite with 10 wt % **FD** POS. This sample was very difficult to mold into quality films for testing. The poor quality of the films tested may lead to the scatter seen in the data, and possibly the lower temperature for the peak in the loss modulus curve. For this study, the glass transition temperature of the polymer is defined as the peak in the loss modulus curves. The addition of fluorinated POS to PCTFE decreases the glass transition temperature by approximately 2 °C. The variation in glass transition temperature seen with the addition of fluorinated POS is small enough to be statistically insignificant.

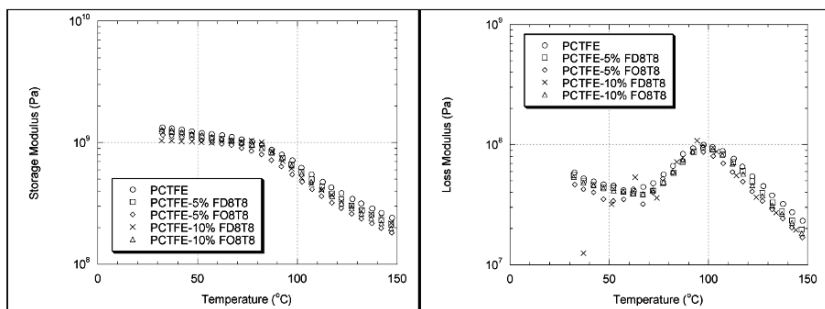


Fig. 6.13 Storage and loss modulus data for FD POS/PCTFE films

6.3.3.4 Surface Properties

While various fluoropolymers are known for their desirable properties, which include hydrophobicity and a low coefficient of friction, incorporation of fluorinated POS may help to improve these properties even further. Contact angles have been obtained on PCTFE nanocomposites containing **FO** and **FD** POS.

Technologies that may benefit from the blending of fluorinated POS into fluoropolymers include abrasion resistance, lubricity, anti-icing, and non-wetting applications. Figure 6.14 (left) shows a drop of water on the surface of a PCTFE film with a contact angle of 88°. A drop of water on the surface of a PCTFE blend containing 10 wt % **FD** POS (Figure 6.14, right) produced a contact angle of 128°. Hence there is a 40° increase in contact angle with a modest 10 wt % added **FD** POS.

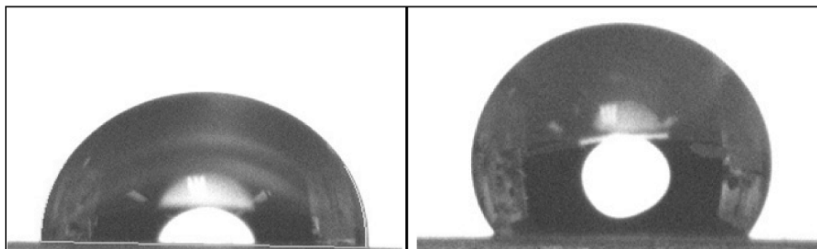


Fig. 6.14 Water contact angles of 88° on PCTFE film (left) and 128° on PCTFE film containing 10 wt % FD POS (right), respectively

Similar to PFCB aryl ether polymer solvent blended coatings carrying **FD** POS, application of hexadecane on the PCTFE melt blended compositions with **FD** POS resulted in improvement of oleophobicity, with hexadecane contact angles increasing from approximately 32° to 58°.

6.4 Conclusions

Various fluorinated polyhedral oligomeric silsesquioxanes (POS) have been solvent or melt blended into a variety of fluoropolymers. These fluoropolymers include perfluorocyclobutyl (PFCB) aryl ether polymers and poly(chlorotrifluoroethylene) (PCTFE). The composite blends produce well-dispersed fluorinated POS based on microscopy analysis. The fluoroalkyl groups on the fluorinated POS cages demonstrate good miscibility in selected fluoropolymer matrices. These fluorinated POS fluoropolymer composites may be useful as low friction surfaces either as bulk components or coatings. Contact angle measurements of the POS fluoropolymers show an improvement of water and hexadecane contact angles over the unfilled materials. The low surface energy POS compounds also appear to act as a processing aid during fluoropolymer processing, significantly reducing both the torque and load measurements in the extruder. Thermal and mechanical properties of the blended fluoropolymers do not compromise the integrity of the unfilled polymers. Work continues to encompass fluorinated POS as simple drop-in modifiers for fluoropolymers. It is also worth noting that fluorinated Si_8O_{12} compounds have recently been used to develop non-wetting and stain resistant fabrics [25] and fabrics with tunable oleophobicity [26].

6.5 Acknowledgments

We gratefully acknowledge the Air Force Research Laboratory, Propulsion Directorate and the Air Force Office of Scientific Research for their financial support. The authors also wish to thank Brian Moore at AFRL for his assistance with AFM images and Marietta Fernandez at AFRL for help with SEM images.

6.6 References

1. Gakh AA, Tuinman AA, Adcock JL, Sachleben RA, Compton RN (1994) *J Am Chem Soc* 116:819.
2. Fagan PJ, Krusic PJ, McEwen CN, Lazar J, Holmes-Parker D, Herron N, Wasserman E (1993) *Science* 262:404.
3. Taylor R, Avent AG, Dennis TJ, Hare JP, Kroto HW, Walton DRM (1992) *Nature* 355:275.
4. Herzog A, Callahan RP, Macdonald CLB, Lynch VM, Hawthorne MF, Lagow RJ (2001) *Angew Chem Int Ed* 40:2121.
5. Hayashi T, Terrones M, Scheu C, Kim YA, Rühle M, Nakajima T, Endo M (2002) *Nano Lett* 2:491.
6. Gonzalez RI, Phillips SH, Hoflund GB (2000) *J Spacecraft and Rockets* 37:463.
7. Phillips SH, Haddad TS, Tomczak SJ (2004) *Curr Opin Solid State Mater Sci* 8:21.
8. POSS[®] is a registered trademark of Hybrid Plastics Inc., Hattiesburg, MS 39401.
9. Li G, Wang L, Hanli N, Pittman CU Jr. (2001) *J Inorg Organomet Polym* 11:123.
10. Hoflund GB, Gonzalez RI, Phillips SH (2001) *J Adhesion Sci Technol* 15:1199.
11. Gilman JW, Schlitzer DS, Lichtenhan JD (1996) *J Appl Polym Sci* 60:591.
12. Lu S-Y, Hamerton I (2002) *Prog Polym Sci* 27:1661.

13. Lee GZ, Wang L, Toghiani H, Daulton TL, Pittman CU Jr. (2002) *Polymer* 43:4167.
14. Zhang W, Fu BX, Schrag E, Hsiao B, Mather PT, Yang N-L, Xu D, Ade H, Rafailovich M, Sokolov J (2002) *Macromolecules* 35:8029.
15. Fu BX, Gelfer MY, Hsiao BS, Phillips S, Viers B, Blanski R, Ruth P (2003) *Polymer* 44:1499.
16. Deng J, Polidan JT, Hottle JR, Farmer-Creely CE, Viers BD, Esker A (2002) *J Am Chem Soc* 124:15194.
17. Fu BX, Hsiao BS, White H, Rafailovich M, Mather PT, Jeon HG, Phillips S, Lichtenhan J, Schwab J (2000) *Polym Int* 49:437.
18. Mabry JM, Vij A, Iacono ST, Viers BD (2008) *Angew Chem Int Ed* 47:4137.
19. Iacono ST, Grabow W, Vij A, Smith DW Jr., Mabry JM (2007) *Chem Commun* 47:4992.
20. Iacono ST, Budy SM, Jin J, Smith DW Jr. (2007) *J Polym Sci Part A Polym Chem* 45:5707.
21. Young T (1805) *Phil Trans Roy Soc* 95:65.
22. Wenzel RN (1936) *Ind Eng Chem* 28:988.
23. Cassie ABD, Baxter S (1944) *Trans Faraday Soc* 40:546.
24. Hong Y, Cooper-White JJ, Mackay ME, Hawker CJ, Malmstrom E, Rehnberg N (1999) *J Rheol* 43:781.
25. Misra R, Cook RD, Morgan SE (2010) *J Appl Polym Sci* 115(4):2322-2331.
26. Choi W, Tuteja A, Chatre S, Mabry JM, Cohen RE, McKinley GH (2009) *Adv Mater* 21(21):2190-2195.